Internal eigenstate problem: The trial state method

Georges Jolicard and John P. Killingbeck
Laboratoire d'Astrophysique de l'Observatoire de Besançon (CNRS UPRESA6091), 41 bis Avenue de l'Observatoire, BP 1615, 25010 Besançon Cedex, France

Marie-Yvonne Perrin
Laboratoire d'Energétique Moléculaire et Macroscopique Combustion du CNRS et de l'ECP, 92295 Chatenay-Malabry, France
(Received 28 April 2000; published 12 January 2001)

It is shown that the device of adding a special trial state to a basis set, thus augmenting by 1 the dimension of any complex matrix being studied, leads to a formalism that permits the application of the wave operator approach to calculating the internal spectrum of the matrix as well as the action of the resolvent operator $(E-H)^{-1}$ on an arbitrary vector in the original N-dimensional space. Two calculational variants of the method are described and both are tested by studying the problem of a short laser pulse interacting with a H_2^+ ion.

DOI: 10.1103/PhysRevE.63.026701 PACS number(s): 02.70.−c

I. INTRODUCTION

Studies of the bound and resonance states of molecular systems and of the quantum dynamical processes involving such systems are often faced with the task of calculating several internal eigenvalues and eigenvectors for large matrices which may have complex elements. This task arises, for example, in the work of Manthe and Miller [1,2], which uses a reaction probability operator expressed in terms of the Green operator [3] for a case in which the potential incorporates a complex absorbing term to enforce outgoing wave boundary conditions in the reactant and product spatial regions. It also arises in the Floquet treatment of photoreactive processes [4,5] which, when allied with the complex coordinate method [6], allows calculation of photoionization and photodissociation probabilities using Floquet eigenvectors as a basis in a generalized Hilbert space; the method can be generalized to nonperiodic systems in order to treat processes involving pulsed laser fields [7]. Recent work [8] shows that strongly nonlinear photodissociation phenomena can be treated by means of a few Floquet eigenvectors in an appropriately defined extended Hilbert space.

The matrices used to describe resonance states and photoreactive processes are often non-Hermitian because of the use of complex rotations or complex absorbing potentials in the calculation of the matrix elements. They are, however, often sparse matrices, for which only the spectrum in a window centered on some reference energy is required or for which only eigenvectors with some suitable property are sought. For example, spectroscopic calculations may need energies that have zero or very small imaginary part (bound states or long-lived resonances), while photoreactive studies primarily select Floquet eigenstates that have a suitably large overlap with some specified initial state.

The many methods of eigenvalue calculation proposed in the literature can be roughly classified into indirect and direct methods. The indirect methods include the relaxation method [9], the spectral method [10], and the filter diagonalization method [11]. The direct methods, which include perturbative and moment method approaches, include those of Bloch [12] and Davidson [13] and the Lanczos and block Lanczos methods [14,15]. Experience with the direct methods has shown, despite their wide range of applicability, some cases for which they typically encounter difficulties. The Bloch algorithm is easily implemented but as a perturbative method it suffers from convergence problems, although these have been somewhat reduced by the use of the intermediate space concept [16] and of quasiquadratic iterative processes [17]. The single-vector Lanczos method shares with the Bloch algorithm and with the method of variational Rayleigh iteration [18] the advantage of requiring only the formation of matrix-vector products but it generates artificial repetitions in the spectrum and tends to converge most readily to eigenvalues at the ends of the spectrum unless special steps are taken to handle these problems. Nevertheless, the Lanczos method does converge quickly for interior eigenvalues, if the local gap spacings are sufficiently large.

Hybrid techniques have been proposed in order to overcome some of the typical defects of the methods mentioned above and so make possible the inspection of any desired part of the spectrum of a large matrix, in what may be appropriately described as ''matrix spectroscopy'' [19]. To this end the Lanczos method has been coupled with a spectral filter [19] and a preconditioned Green function block Lanczos algorithm has also been proposed [20]. A Green function expansion in terms of Chebyshev polynomials, exploiting their simple recurrence relations, was used in [21]. Chebyshev polynomials are also used in a spectral projection method, which uses an absorbing potential-like damping factor and is able to produce simultaneous results at several energies; this last approach has been applied to reactive scattering problems [22] and to calculations of vibrational resonances [23].

The present work tests an approach that blends a Green function filter with wave operator techniques. The strategy used hinges on an equivalence between two calculations, first, that of finding the resolvent $(E-H)^{-1}V$ for an arbitrary vector V in the primary N-dimensional Hilbert space and, second, that of solving an eigenvalue problem in an augmented space of $N+1$ dimensions for a new matrix that depends linearly on H. The $(N+1)$-dimensional space is obtained by adding a special ''trial state'' to the original space,

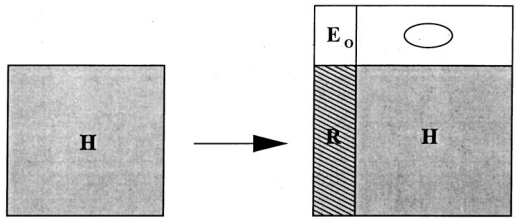

FIG. 1. Schematic representation of the modification of the H matrix that is produced by introducing a single extra test state which is nonsymmetrically coupled to the states in the original Hilbert space.

and the new eigenvalue problem is solved by using a time-dependent wave operator formalism which has been described and applied in previous work [24].

The formalism is given in detail in Sec. II, while Sec. III sets out two calculational implementations of it: one of them proceeds by working out $(E-H)^{-1}V$, while the other aims more directly at the eigenvalues. Section IV carries out a numerical trial of these two implementations by calculating some generalized Floquet eigenstates for the problem of a strong pulsed laser field interacting with the H_2^+ ion.

II. THE BASIC IDEA

Let H be a general $(N\times N)$ nonsingular matrix representing some Hamiltonian in a finite N-dimensional Hilbert space and $|\alpha\rangle$ a vector of this space. H can be a complex non-Hermitian matrix if complex similarity transformations have been intoduced to give a representation of any continua involved in the processes described.

If H is partitioned into a zeroth-order Hamiltonian plus a perturbation, $(H=H_0+V)$, and $|\alpha\rangle$ is an eigenvector of H_0, then a key problem in quantum dynamics is the calculation of the H eigenvector $|\lambda_\alpha\rangle$ that issues from $|\alpha\rangle$ when an adiabatic switching on of the perturbation V is used. In the strong coupling regime, the calculation principally involves the group of n H eigenvectors $n\ll N$ $\{|\lambda_\alpha^i\rangle, i=1-n\}$ that have significant overlap with the initial state $|\alpha\rangle$.

An indirect way to treat the problem is to form the product $[1/(E-H)]|\alpha\rangle$ in the N-dimensional Hilbert space ε_N. In the spectral projection method of Mandelshtam and Taylor [22] this product is found by using a polynomial expansion of the resolvent operator. The alternative approach of the present work introduces an extended $(N+1)$-dimensional Hilbert space ε_{N+1} consisting of the direct sum of ε_N and a one-dimensional supplementary space spanned by a vector $|0\rangle$ orthogonal to ε_N. This vector, the test state is a mathematical aid, with no direct physical interpretation. In the extended space we introduce a new nonsymmetric matrix $\mathcal{H}$ with a structure that is displayed pictorially in Fig. 1. This matrix has a first column containing a single arbitrary diagonal matrix element E_0 and the vector R, shown in Fig. 1, which can be seen to represent the formal operator

$$\mathcal{R}=|\alpha\rangle\langle 0| \tag{1}$$

if the numerical elements inserted in the column R are those of the vector $|\alpha\rangle$.

This matrix possesses two main features: (i) All the nondiagonal elements in the first row are zero; the diagonal element E_0 is consequently an exact eigenvalue of the new $(N+1)\times(N+1)$ matrix, whatever the elements are in the first column. (ii) The matrix is non-Hermitian, even if H is a real symmetric matrix.

The last point is a handicap since the eigenvalue treatment of this matrix cannot use the well established procedures for Hermitian matrices. However, the matrix has an interesting property related to the eigenvector associated with E_0. An elementary calculation reveals that this eigenvector $|\lambda_0\rangle$ can be expressed in the form

$$|\lambda_0\rangle=\left[1+\left(\frac{1}{E_0-H}\right)\mathcal{R}\right]|0\rangle \tag{2}$$

and this provides the key point of our calculational strategy. To see this result we set the first eigencolumn element equal to 1 and regard the remaining elements as a vector $|X\rangle$. The eigenvalue equation gives for the Jth component

$$R_J\times 1+\sum_K H_{JK}X_K=E_0X_J,$$

leading to the vector equations

$$[(E_0\mathbf{1}-H)X]_J=R_J,$$

i.e.,

$$|X\rangle=(E_0-H)^{-1}|R\rangle,$$

which is equivalent to Eq. (2), since we choose $|R\rangle=|\alpha\rangle$. Consequently we find from Eqs. (1) and (2) that the nondiagonal components of vector $|\lambda_0\rangle$ are given by

$$(|\lambda_0\rangle)_{\text{off diag}}=\frac{1}{E_0-H}|\alpha\rangle, \tag{3}$$

so that the calculation of the action of the resolvent operator on the trial vector $|\alpha\rangle$ can be found by solving the eigenvalue equation

$$\mathcal{H}|\lambda_0\rangle=E_0|\lambda_0\rangle \tag{4}$$

in the extended space.

This offers the possibility of applying a standard eigenvalue algorithm to solve this filtered system, albeit still with the restriction that $\mathcal{H}$ is a non-Hermitian matrix. The extra state $|0\rangle$ which gives its name to this method was initially called the ''état sonde'' in French; in English it is best rendered as trial state (or probe state).

At first sight it might appear that the reformulation of the problem has not changed the intrinsic difficulty of its solution. However, the modified formulation brings the problem within the region of applicability of the time-dependent wave operator formalism [24], which can handle Eq. (4) when E_0 is a fixed number and when $|\lambda_0\rangle$ has an $|X\rangle$ component that develops from an initial vector $|\alpha\rangle$ in the space ε_N.

III. PRACTICAL IMPLEMENTATION

A. The general scheme

From Eqs. (2) and (3), the solution $|\lambda_0\rangle$ of the eigenvalue problem $\mathcal{H}|\lambda_0\rangle = E_0|\lambda_0\rangle$, Eq. (4), can be written as

$$|\lambda_0\rangle = |0\rangle + |X\rangle, \tag{5}$$

where

$$|X\rangle = \frac{1}{E_0 - H}|\alpha\rangle \tag{6}$$

designates the components of the eigensolution in the primary Hilbert space ε_N.

Denoting by $|\lambda_\beta\rangle$ the eigenvectors of H and by E_β their associated eigenvalues, we have in the general case

$$|\alpha\rangle = \sum_\beta a_\beta |\lambda_\beta\rangle \tag{7}$$

and

$$|X\rangle = \sum_\beta \frac{a_\beta}{E_0 - E_\beta}|\lambda_\beta\rangle. \tag{8}$$

We particularly note that when the trial vector $|\alpha\rangle$ is proportional to a single eigenvector $|\lambda_\alpha\rangle$, i.e., $|\alpha\rangle = a_\alpha|\lambda_\alpha\rangle$, then $|X\rangle$ is itself proportional to this vector: $|X\rangle = [a_\alpha/(E_0 - E_\alpha)]|\lambda_\alpha\rangle$. This special feature will be used later.

We will now integrate the eigenvalue equation (4) by noting that $|\lambda_0\rangle$ satisfies an intermediate normalization condition in the extended Hilbert space, i.e., $\langle 0|\lambda_0\rangle = 1$. Consequently, $|\lambda_0\rangle\langle 0|$ can be assimilated to the Bloch wave operator associated with the test state $|0\rangle$ and the matrix $\mathcal{H}$. The calculation of the off-diagonal part X of this operator [i.e., $X = \Sigma_{j\neq 0}(\langle j|\lambda_0\rangle)|j\rangle\langle 0|$] can be made by using the time-dependent wave operator formulation already explained in [24]. We will briefly describe that formalism and its adaptation for the present problem.

(i) First we select a trial wave operator $|X^{(n=0)}\rangle$. The simplest choice is $|X^{(n=0)}\rangle = 0$. However, if $|\alpha\rangle$ is one of the H_0 eigenvectors then a better choice is

$$|X^{(n=0)}\rangle = \frac{1}{E_0 - H_{\alpha\alpha}}|\alpha\rangle \tag{9}$$

[cf. Eq. (6)].

(ii) The matrix $\mathcal{H}$ is then separated into two parts,

$$\mathcal{H} = (\mathcal{H} - Q_0\tilde{\mathcal{H}}^{(n=0)}P_0) + Q_0\tilde{\mathcal{H}}^{(n=0)}P_0, \tag{10}$$

where $\tilde{\mathcal{H}}^{(n=0)} = (1 - X^{(n=0)})\mathcal{H}(1 + X^{(n=0)})$. Here P_0 is the projector $|0\rangle\langle 0|$ for the test case $|0\rangle$ and Q_0 is the projector for the complementary space, i.e., for the primary Hilbert space ε_N.

(iii) An adiabatic integration procedure is then introduced by taking a time-dependent matrix in place of the second matrix on the right hand side of Eq. (10):

$$Q_0\tilde{\mathcal{H}}^{(n=0)}P_0 \rightarrow Q_0\tilde{\mathcal{H}}^{(n=0)}P_0\left[\frac{t}{T_s} - \frac{1}{2\pi}\sin(2\pi t/T_s)\right]. \tag{11}$$

This introduces artificially a time-dependent matrix $\mathcal{H}(t)$ by replacing the first column $R = |\alpha\rangle\langle 0|$ with a time-dependent one such that at $t=0$ the trial vector $|0\rangle + |X^{(n=0)}\rangle$ is an exact eigenvector of $\mathcal{H}(t=0) = \mathcal{H} - Q_0\tilde{\mathcal{H}}^{(n=0)}P_0$, while at $t = T_s$ we have $\mathcal{H}(t=T_s) = \mathcal{H}$. The switching function $F(t) = t/T_s - (1/2\pi)\sin(2\pi t/T_s)$ increases from 0 at $t=0$ up to 1 at $t = T_s$ with zero first- and second-order time derivatives at the ends of the interval in order to reduce nonadiabatic effects.

(iv) The evolution equation for the time-dependent reduced wave operator is then integrated over the interval $[0, T_s]$ by taking the initial choice

$$X(t=0) = X^{(n=0)}. \tag{12}$$

The integration process uses the formula derived in [24],

$$X(t+\Delta t) = X(t) + \left[X(t-\Delta t) - X(t) + \frac{Q_0\tilde{\mathcal{H}}(t)P_0}{\hbar\omega}\right] \times \exp(-2i\omega\Delta t) - \frac{Q_0\tilde{\mathcal{H}}(t)P_0}{\hbar\omega}, \tag{13}$$

where the compact notation $\omega_{j,\alpha} = (\tilde{\mathcal{H}}_{jj} - \tilde{\mathcal{H}}_{\alpha\alpha})/\hbar$ has been used.

The propagation equation (13) has desirable interpolatory properties. The limit $\omega \rightarrow 0$ leads to the standard second-order differential scheme [25], while in the region of large ω the rapidly oscillating term has a negligible contribution at the adiabatic limit ($T_s \rightarrow \infty$) and can be suppressed, leading to a result similar to the RDWA iteration scheme result: $X(t+\Delta t) = X(t) - [Q_0\tilde{\mathcal{H}}(t)P_0]/\hbar\omega$. Equation (13) is thus appropriate for the adiabatic limit (i.e., the case of large switching time T_s) since the high-frequency terms, which usually produce an instability and so impose the need for a large number of time steps, can be arbitrarily suppressed. The equation can also cope with accidental resonances ($\omega \sim 0$) between the states that are implicitly involved in the integration process.

The integration of this time-dependent wave operator on $[t=0,\ t=T_s]$ gives a solution $X^{(n+1)}$, a first-cycle solution, which for sufficiently large T_s will be a good approximation of the exact stationary wave operator. When the nonadiabatic effects remain too large, i.e., when the residual term $Q_0\tilde{\mathcal{H}}^{(n+1)}P_0 = Q_0(1 - X^{(n+1)})\mathcal{H}(1 + X^{(n+1)})$ is not sufficiently small, a second cycle of integration [Eqs. (10)–(13)] can be performed by simply incrementing the index n ($n = 0 \rightarrow n = 1$) in the procedure (i)→(iv).

B. A second option: The eigenvalue problem

The preceding cycle of integration converges to the solution $|\lambda_0\rangle = |0\rangle + [1/(E_0 - H)]|\alpha\rangle$. From Eqs. (7) and (8), it gives a vector $|\lambda_0\rangle$ that is a linear combination of the exact H eigenvectors $|\lambda_\beta\rangle$ possessing a nonvanishing overlap with $|\alpha\rangle$. When the chosen value of E_0 is far away from the corresponding eigenvalues E_β in the complex plane, the integration is easier but the final solution has a wide distribution over the basis set $|\lambda_\beta\rangle$. In contrast, when E_0 is near to a group of N_0 exact eigenvalues, the weight of these states

increases dramatically in the expansion [Eq. (8)] because of the large factors $1/(E_0-E_\beta)$. By using N_0 different E_0 values in this region of the complex plane one can generate an $N_0\times N_0$ effective Hamiltonian which when diagonalized will give the group of vectors $|\lambda_\beta\rangle$ involved in the expansion.

However, our formalism can actually be modified to solve the eigenproblem $H|\lambda_\alpha\rangle=E_\alpha|\lambda_\alpha\rangle$ directly and not just to find the product $[1/(E_0-H)]|\alpha\rangle$ for the indirect process of the preceding paragraph. To simplify the presentation we shall assume that $|\alpha\rangle$ is one of the basis vectors used in the representation of H. An adiabatic scheme is then introduced by transforming H into a time-dependent matrix,

$$H\rightarrow H(t). \tag{14}$$

In this process all the matrix elements are unchanged except the off-diagonal elements of column α, in which we incorporate the time-dependent factor:

$$f(t)=\left[\frac{t}{T_s}-\frac{1}{2\pi}\sin\left(\frac{2\pi t}{T_s}\right)\right]. \tag{15}$$

With this choice $|\alpha\rangle$ is an eigenvector of $H(t=0)$ with the eigenvalue $E^0_\alpha=\langle\alpha|H|\alpha\rangle$, while $H(t=T_s)\equiv H$. The initial wave operator associated with the test state is chosen to be

$$|\lambda_0(t=0)\rangle\langle 0|=|0\rangle\langle 0|+|X(t=0)\rangle\langle 0|, \tag{16}$$

with

$$|X(t=0)\rangle=\frac{1}{E_0-H(t=0)}|\alpha\rangle=\frac{1}{E_0-H_{\alpha\alpha}}|\alpha\rangle,$$

i.e., we use $|\alpha\rangle$ as the initial R column (cf. Fig. 1).

The eigenvalue equation $\mathcal{H}|\lambda_0\rangle=E_0|\lambda_0\rangle$ is then integrated by using the time-dependent wave operator procedure and by forcing at each time a proportionality between $|\lambda_0(t)\rangle$ and the $H(t)$ eigenvector $|\lambda_\alpha(t)\rangle$ that issued from $|\alpha\rangle$ at time $t=0$. This proportionality is imposed by varying the first column as follows (Fig. 1):

$$\mathcal{R}(t)=\sum_{j\neq 0}\{[E_0-E_\alpha(t)]\langle j|\lambda_0(t)\rangle\}|j\rangle\langle 0|, \tag{17}$$

where

$$E_\alpha(t)=\langle X(t)|HX(t)\rangle/\langle X(t)|X(t)\rangle.$$

This forced evolution is introduced in order to obtain at the end of the integration using Eq. (13) a vector $|X\rangle$ that is proportional to $|\lambda_\alpha\rangle$, i.e., to ensure that $|X(t=T_s)\rangle=[1/(E_0-E_\alpha)]|\lambda_\alpha\rangle$, with $H|\lambda_\alpha\rangle=E_\alpha|\lambda_\alpha\rangle$. The procedure is identical to those in the preceding section, except that two columns [first column of Eq. (17) and column α of Eq. (15)] are now modified during the time integration.

IV. TEST: CALCULATION OF FLOQUET EIGENSTATES TO DESCRIBE PHOTODISSOCIATION DUE TO ULTRASHORT LASER PULSES

We will consider the case of the $H_2{}^+$ molecule subjected to a short Gaussian electric field pulse. In the Born-Oppenheimer approximation, the coupling produced by the field-matter interaction is

$$V_{gu}(r,t)=\mu_{gu}(r)E_0\exp[-(t-t_0)^2/\mathcal{T}^2]\cos(\omega_0 t), \tag{18}$$

where E_0 is the maximum amplitude of the electric field and μ_{gu} is the transition moment between the ground electronic surface $1s\sigma_g$ and the excited $2p\sigma_u$ surface.

The (t,t') wave operator theory [8] sets out to describe the photodissociation process induced by a short laser pulse by using a reduced basis formed by a few eigenvectors of the Floquet Hamiltonian

$$H_F(t)=H(t)-i\hbar\frac{\partial}{\partial t}. \tag{19}$$

The Hamiltonian $H(t)$ represents the dynamics of the molecule on the two surfaces coupled by the field. It includes a negative imaginary potential $-iV_{\rm opt}(r)$ added in the spatial asymptotic region to absorb the outgoing wave packets. This Hamiltonian belongs to an extended Hilbert space which includes the two radial coordinates for the two surfaces and the whole time variation of the field envelope. This space is spanned by a discrete product basis set with elements $|j\rangle\otimes|n\rangle$, where $|j\rangle$ are the eigenvectors of H without the field coupling [Eq. (18)] and $|n\rangle$ is a basis that spans a time interval $[-T/2,T/2]$ in which the Gaussian field envelope is included and with elements $\langle t|n\rangle=\exp(2\pi int/T)$.

Using the (t,t') wave operator theory [8], one can express the photoreactive dynamics issuing from an initial unperturbed eigenstate such as $|j=1\rangle\times|n=0\rangle$ (i.e., the first free eigenstate of the ground surface times the initial laser field state $|n=0\rangle$) by simply calculating the associated Floquet eigenstate ($|\lambda_{j=1,n=0}\rangle$). The eigenproblem in the generalized Hilbert space then appears as the key aspect of this formulation. The present test calculation considers the same data as those of [24]. In Eq. (18) ω_0 is taken to be that corresponding to a wavelength $\lambda=329.7$ nm, to induce an energetically favorable vertical three-photon transition from the bound state ($1s\sigma_g$, $v=0$) to the continuum ($2p\sigma_u$). The field amplitude E_0 corresponds to a laser field intensity of 2.5×10^{13} W/cm^2.

2×100 eigenfuctions $|j\rangle$ are used to represent the two uncoupled surfaces on the range [0,12] a.u. of the radial coordinate and 198 functions $|n\rangle$ are used to span the time interval $[-T/2,T/2]$ with $T=1000$ a.u. (On this interval the Gaussian pulse with $\mathcal{T}=140$ a.u. [Eq. (18)] is centered at $t=0$.) This leads to a coupled basis that includes 39 600 states.

Figure 2 represents the initial unperturbed eigenvalue $E^0_{j=1,n=0}$ (situated at the bottom of the arrow) and the first 500 nearest unperturbed eigenvalues. The optical potential displaces all these eigenvalues into the lower half of the complex E plane. Nevertheless, the density of states remains high, with multiple near degeneracies. The test state eigenvalue E_0 is defined from the initial eigenvalue by using a complex positive shift

$$E_0=E^0_{j=1,n=0}+i\Delta. \tag{20}$$

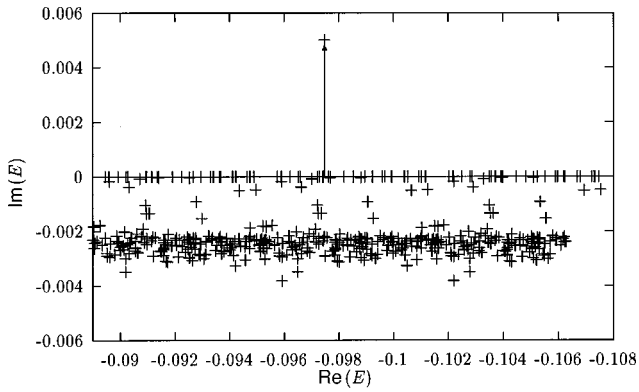

FIG. 2. Positions in the complex plane of the unperturbed Floquet eigenvalues for the problem of H_2^+ subjected to a Gaussian pulse (see the text). The units are atomic units. The arrow connects the initial unperturbed state eigenvalue $E^0_{j=1,n=0}$ to the test state energy E_0. The 500 nearest unperturbed eigenvalues are also represented.

Figure 2 refers to the choice $\Delta = 0.5\times 10^{-2}$. This shift process extracts the test state from the region of large density of states by moving E_0 into the upper half plane. It thus avoids accidental resonances, since all the exact H eigenvalues $E_{j,n}$ as well as all the unperturbed eigenvalues $E^0_{j,n}$ are situated in the lower half plane.

Figure 3 presents some results obtained by applying the computational method of Sec. III A. This figure shows on a logarithmic scale a measure of the ''defect'' of the calculated test state $|\lambda_0\rangle$ [Eq. (5)] with respect to the exact eigenvector. The measure chosen is the quantity

$$\|(\mathcal{H}-E_0)|\lambda_0\rangle\|^2. \tag{21}$$

The independent variable used in Fig. 3 is the ''order of iteration'' in the wave operator time integral [Eq. (13)], i.e., the number of calls of the subroutine which forms the product of the $\mathcal{H}$ matrix with the vector $|X(t)\rangle$ (this number of calls gives an approximate measure of the total CPU time required).

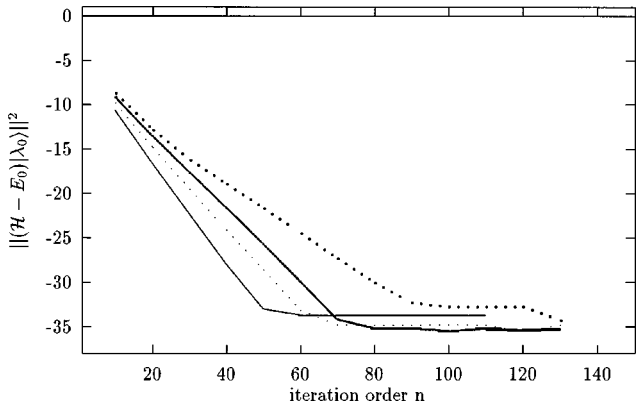

FIG. 3. A measure of the defect of the calculated test state $|\lambda_0\rangle$ as an eigenvector of the extended matrix $\mathcal{H}$, $\|(\mathcal{H}-E_0)|\lambda_0\rangle\|^2$, is shown on a logarithmic scale as a function of the iteration order n. Four curves, corresponding to four decreasing values of the complex shift $i\Delta$ [Eq. (20)] are represented. From the bottom (full line), to the top (dotted line): $\Delta = 10^{-1}$, 0.3×10^{-1}, 10^{-2}, 0.3×10^{-2}.

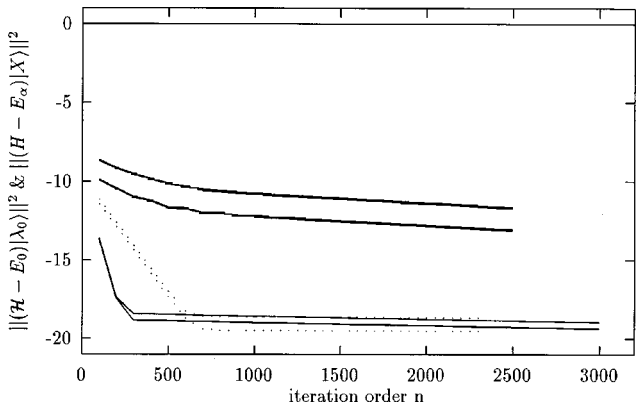

FIG. 4. Convergence rate for the solution of the eigenvalue problem $(H-E_\lambda)|X\rangle = 0$ when using the procedure described in Sec. III B. Three pairs of curves corresponding to three increasing values of Δ are presented: full lines, $\Delta = 0.5\times 10^{-2}$; dashed lines, $\Delta = 10^{-2}$; dotted lines, $\Delta = 0.5\times 10^{-1}$. For each pair the lower curve is a measure of the defect of $|\lambda_0\rangle$ as an eigenvector of $\mathcal{H}$, i.e., $\|(\mathcal{H}-E_0)|\lambda_0\rangle\|^2$. The upper curve is a measure of the defect of $|X\rangle$ [Eq. (5)] as an eigenvector of H.

Curves corresponding to four decreasing values of the shift Δ [Eq. (20)] are shown. The convergence is relatively fast. A precision of 10^{-20} is obtained after 30 iterations for the largest Δ value, although decreasing Δ decreases the rate of convergence. This effect would be anticipated, since the form of Eq. (13) implies that decreasing Δ will introduce more and more small frequencies ω into the equation of propagation. For Δ values smaller than 0.3×10^{-2} a significant increase of the number of time steps (and thus a decrease of Δt) is required to produce convergence. (In the case of Fig. 3, each cycle between $t=0$ and T_s was made using only ten time steps.)

Figure 4 presents results that relate to the eigenvalue option presented in Sec. III B. Three pairs of curves are presented for three decreasing values of the shift Δ. For each Δ value two curves are shown. In each case the lowest curve corresponds to the measure of the defect of $|\lambda_0\rangle$ as an eigenvector of $\mathcal{H}$, i.e., the quantity $\|\mathcal{H}-E_0)|\lambda_0\rangle\|^2$ [Eq. (21)], where $\mathcal{H}$ represents the value of the matrix at the end of the cycle: $t=T_s$. The upper curve is a measure of the defect of $|X(t=T_s)\rangle$ [i.e., the part of $|\lambda_0(t=T_s)\rangle$ embedded in the original Hilbert space ϵ_N] as an eigenvector of the matrix H,

$$\|(H-E_\alpha)|X(T_s)\rangle\|^2. \tag{22}$$

This figure reveals that the concepts introduced in the eigenvalue option (Sec. III B) are appropriate. It is in fact possible to impose a proportionality between $|X(t)\rangle$ [Eq. (5)] and $|\lambda_\alpha(t)\rangle$ and thus to follow adiabatically the instantaneous H eigenvector $|\lambda_\alpha(t)\rangle$, although the concomitant penalty for this is a decrease of the rate of convergence. The difference in the behavior of $\|(\mathcal{H}-E_0)|\lambda_0\rangle\|^2$ at $\Delta = 10^{-2}$, as produced by changing between the two methods set out in Sec. III, is clearly illustrated by Figs. 3 and 4.

The results clearly become incorrect when Δ is too large (e.g., at $\Delta = 0.05$). This is simply because in this case E_0 is far away from the selected unperturbed eigenvalue $E^0_{j=1,n=0}$

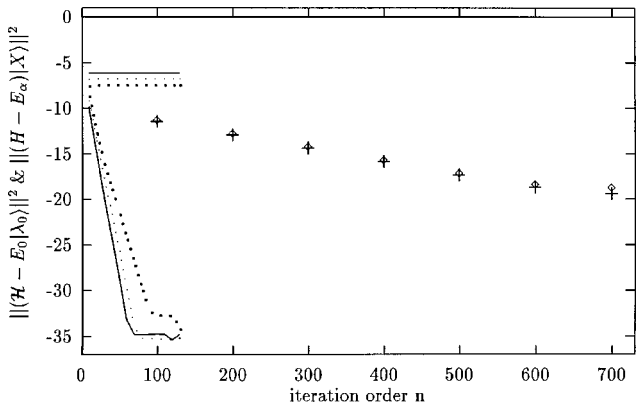

FIG. 5. Comparison of the convergence rates corresponding to the use of the algorithms of Secs. III A and III B (see text). Three pairs of curves correspond to the general scheme (Sec. III A): full lines, $\Delta=0.3\times10^{-1}$; dashed lines, $\Delta=10^{-2}$; dotted lines, $\Delta=0.3\times10^{-2}$. The upper flat lines show $\|(H-E_\alpha)|X\rangle\|^2$ and the lower ones show $\|(\mathcal{H}-E_0)|\lambda_0\rangle\|^2$. The points $\diamond$ and + show $\|(H-E_\alpha)|X\rangle\|^2$ and $\|(\mathcal{H}-E_0)|\lambda_0\rangle\|^2$ at $\Delta=10^{-2}$ for the eigenvalue method of Sec. III B.

and thus far away from the exact H eigenvalue $E_{j=1,n=0}$. With such a large separation it is impossible to force an adiabatic response and the propagated solution $|X(t)\rangle$ spreads out over many eigenvectors $|\lambda_\beta\rangle$.

Figure 5 compares more directly the general scheme (Sec. III A) and the specialized eigenvalue option (Sec. III B). The dashed, dotted, and full lines correspond to the general scheme. For each Δ value, two curves represent successively the two functions $\|(\mathcal{H}-E_0)|\lambda_0\rangle\|^2$ and $\|(H-E_\alpha)|X\rangle\|^2$. In this case the function $\|(H-E_\alpha)|X\rangle\|^2$ converges to large values, particularly when Δ is large. One obtains, for example, a plateau value of about 10^{-6} for $\Delta=0.03$. This means that the test state $|\lambda_0\rangle=|0\rangle+[1/(E_0-H)]|\alpha\rangle$, which is converged to a precision of less than 10^{-30}, has a wide-range expansion over the basis set of H eigenvectors $\{|\lambda_\beta\rangle\}$.

By contrast the two same functions converge to small values (of about 10^{-19} and 10^{-18}) in the case of the eigenvalue option. This indicates that in this case the converged test state $|\lambda_0\rangle$ is, as expected, proportional to a single H eigenvector, i.e., that we have $|\lambda_0\rangle=|0\rangle+[1/(E_0-E_\alpha)]|\lambda_\alpha\rangle$, where α denotes the state $(j=1,\ n=0)$. The figure also shows the decrease of the convergence rate that occurs when the eigenvalue option is used.

V. CONCLUSION

The model of the trial state is based on the use of a convenient mathematical artifact. By increasing by 1 the dimension of the Hilbert space in which H operates, with the creation of a test state nonsymmetrically coupled to the initial H matrix, a new representation of the Green operator equation $|X\rangle=[1/(E-H)]|\alpha\rangle$ is obtained. This reformulation permits the application of various algorithms developed within the framework of stationary and time-dependent wave operator theories. An adaptation of this formulation allows us to solve the eigenvalue problem $|\alpha\rangle\rightarrow|\lambda_\alpha\rangle$ for internal eigenstates.

The algorithm used here for the eigenvalue problem will remain applicable to general non-Hermitian matrices, but the modification introduced to impose adiabatic following of the instantaneous eigenvectors was seen to give a marked reduction in the convergence rate. We are currently exploring methods that can be used to counter this effect.

[1] U. Manthe and W. H. Miller, J. Chem. Phys. **99**, 3411 (1993).
[2] A. Viel, C. Leforestier, and W. H. Miller, J. Chem. Phys. **108**, 3489 (1998).
[3] T. Seideman and W. H. Miller, J. Chem. Phys. **96**, 4412 (1992).
[4] J. H. Shirley, Phys. Rev. B **138**, 979 (1965).
[5] S. I. Chu, Adv. Chem. Phys. **73**, 739 (1989).
[6] N. Ben-Tal, N. Moiseyev, C. Leforestier, and R. Kosloff, J. Chem. Phys. **94**, 7311 (1991).
[7] U. Peskin and N. Moiseyev, J. Chem. Phys. **99**, 4590 (1993).
[8] G. Jolicard and N. Balakrishnan, J. Chem. Phys. **106**, 3613 (1997).
[9] R. Kosloff and H. Tal-Ezer, Chem. Phys. Lett. **127**, 223 (1986).
[10] M. D. Feit, J. A. Fleck, and A. Steiger, J. Comput. Phys. **47**, 412 (1982).
[11] D. Neuhauser, J. Chem. Phys. **93**, 2611 (1990); **95**, 4927 (1991).
[12] C. Bloch, Nucl. Phys. **6**, 329 (1958); Ph. Durand, Phys. Rev. A **28**, 3184 (1983).
[13] E. R. Davidson, Comput. Phys. Commun. **53**, 49 (1989).
[14] C. Lanczos, J. Res. Natl. Bur. Stand. **45**, 255 (1950).
[15] G. H. Golub and R. Underwood, in *Mathematical Software III*, edited by J. Rice (Academic, New York, 1977); R. G. Grimes, J. G. Lewis, and H. D. Simon, SIAM J. Matrix Anal. Appl. **15**, 228 (1994).
[16] Ph. Durand and J. P. Malrieu, in *Ab Initio Methods in Quantum Chemistry I*, edited by K. P. Lawley (Wiley, New York, 1987), p. 352; Ph. Durand and I. Paidarová, Phys. Rev. A **58**, 1867 (1998).
[17] Ph. Durand, I. Paidarová, G. Jolicard, and F. Gemperle, J. Chem. Phys. **112**, 7363 (2000).
[18] J. P. Killingbeck and G. Jolicard, Chem. Phys. Lett. **255**, 79 (1996).
[19] R. E. Wyatt, Phys. Rev. E **51**, 3643 (1995); J. Chem. Phys. **103**, 8433 (1995).
[20] T. J. Minehard, J. D. Adcock, and R. E. Wyatt, Phys. Rev. E **56**, 4837 (1997).
[21] V. A. Mandelshtam and H. S. Taylor, J. Chem. Phys. **103**, 2903 (1995).
[22] V. A. Mandelshtam and H. S. Taylor, J. Chem. Phys. **102**, 7390 (1995).
[23] T. P. Grozdanov, V. A. Mandelshtam, and H. S. Taylor, J. Chem. Phys. **103**, 7990 (1995); **103**, 10074 (1995).
[24] G. Jolicard, J. P. Killingbeck, A. Grosjean, and J. M. Zucconi, J. Chem. Phys. **111**, 7272 (1999).
[25] C. Leforestier *et al.*, J. Comput. Phys. **94**, 59 (1991).